

# Glutamate Delta-1 Receptor Regulates Metabotropic Glutamate Receptor 5 Signaling in the Hippocampus

Pratyush S. Suryavanshi, Subhash C. Gupta, Roopali Yadav, Varun Keshewani, Jinxu Liu, and Shashank M. Dravid

Department of Pharmacology, Creighton University, Omaha, Nebraska

Received April 19, 2016; accepted May 24, 2016

## ABSTRACT

The delta family of ionotropic glutamate receptors consists of glutamate delta-1 (GluD1) and glutamate delta-2 receptors. We have previously shown that GluD1 knockout mice exhibit features of developmental delay, including impaired spine pruning and switch in the N-methyl-D-aspartate receptor subunit, which are relevant to autism and other neurodevelopmental disorders. Here, we identified a novel role of GluD1 in regulating metabotropic glutamate receptor 5 (mGlu5) signaling in the hippocampus. Immunohistochemical analysis demonstrated colocalization of mGlu5 with GluD1 punctas in the hippocampus. Additionally, GluD1 protein coimmunoprecipitated with mGlu5 in the hippocampal membrane fraction, as well as when overexpressed in human embryonic kidney 293 cells, demonstrating that GluD1 and mGlu5 may cooperate in a signaling complex. The interaction of mGlu5 with scaffold protein effector Homer, which regulates mechanistic target of rapamycin (mTOR)

signaling, was abnormal both under basal conditions and in response to mGlu1/5 agonist (RS)-3,5-dihydroxyphenylglycine (DHPG) in GluD1 knockout mice. The basal levels of phosphorylated mTOR and protein kinase B, the signaling proteins downstream of mGlu5 activation, were higher in GluD1 knockout mice, and no further increase was induced by DHPG. We also observed higher basal protein translation and an absence of DHPG-induced increase in GluD1 knockout mice. In accordance with a role of mGlu5-mediated mTOR signaling in synaptic plasticity, DHPG-induced internalization of surface  $\alpha$ -amino-3-hydroxy-5-methyl-4-isoxazolepropionic acid receptor subunits was impaired in the GluD1 knockout mice. These results demonstrate that GluD1 interacts with mGlu5, and loss of GluD1 impairs normal mGlu5 signaling potentially by dysregulating coupling to its effector. These studies identify a novel role of the enigmatic GluD1 subunit in hippocampal function.

## Introduction

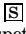
Glutamate delta-1 (GluD1) and glutamate delta-2 (GluD2) constitute the delta subfamily of ionotropic glutamate receptors. GluD1 is widely expressed in the brain, with high levels in the hippocampus (Lomeli et al., 1993; Yadav et al., 2012; Hepp et al., 2014; Konno et al., 2014; Gupta et al., 2015). Among the ionotropic glutamate receptors, delta receptors are unique in that they do not exhibit agonist-induced current in a heterologous expression system. However, GluN1 subunit ligands, such as D-serine and glycine, bind to the ligand-binding domain and induce conformational change in the GluD1 receptor (Naur et al., 2007; Yadav et al., 2011). We have recently shown that loss of GluD1 in a mouse model leads to

abnormal social and emotional behaviors, including social interaction deficits and repetitive behavior (Yadav et al., 2012, 2013; Gupta et al., 2015). We also observed specific cognitive deficits in hippocampus-dependent contextual fear learning and reversal learning in GluD1 knockout (KO) mice (Yadav et al., 2012, 2013). More recently, we have found that loss of GluD1 produces molecular phenotypes relevant to autism and developmental delay, including impaired dendritic spine pruning and switch in N-methyl-D-aspartate (NMDA) receptor GluN2B to the GluN2A subunit in the hippocampus and prefrontal cortex (Grossman et al., 2006; Penzes et al., 2011; Swanger et al., 2011; Gupta et al., 2015). Indeed, single-nucleotide polymorphism and copy-number variation studies have identified the GRID1 gene, which codes for GluD1, as a susceptibility gene for autism, schizophrenia, bipolar disorder, and major depression (Fallin et al., 2005; Glessner et al., 2009; Smith et al., 2009; Greenwood et al., 2011; Nord et al., 2011; Edwards et al., 2012; Griswold et al., 2012).

Recent expression studies demonstrated that the general pattern of GluD1 expression is quite similar to that of

This work was supported by the National Institutes of Health National Institute of Mental Health [Grant R21-MH098270], National Science Foundation [Grant 1456818], Nebraska Department of Health and Human Services [Stem Cell 2014-08], and George-Haddix Faculty Development Funds.

dx.doi.org/10.1124/mol.116.104786.

 This article has supplemental material available at molpharm.aspetjournals.org.

**ABBREVIATIONS:** aCSF, artificial cerebrospinal fluid; Akt, protein kinase B; AMPA,  $\alpha$ -amino-3-hydroxy-5-methyl-4-isoxazolepropionic acid; ANOVA, analysis of variance; ASD, autism spectrum disorder; DHPG, (RS)-3,5-dihydroxyphenylglycine; CHPG, (RS)-2-chloro-5-hydroxyphenylglycine; DL-AP5, DL-2-amino-5-phosphonopentanoic acid; ERK, extracellular signal-regulated kinase; GluD, glutamate delta; HA-GluD1, hemagglutinin-GluD1; HEK293, human embryonic kidney 293; IP, immunoprecipitation; KO, knockout; MeCP2, methyl CpG binding protein 2; mGlu5, metabotropic glutamate receptor 5; MPEP, 2-methyl-6-(phenylethynyl)pyridine; mTOR, mechanistic target of rapamycin; NDS, normal donkey serum; NMDA, N-methyl-D-aspartate; NGS, normal goat serum; PB, phosphate buffer; PBS, phosphate-buffered saline; TBS, Tris-buffered saline.

metabotropic glutamate receptor 5 (mGlu5)—in particular, they are predominantly expressed in the cortex, hippocampus, and striatum in the forebrain region (Shigemoto and Mizuno, 2000; Hepp et al., 2014; Konno et al., 2014). Moreover, at a subcellular level, GluD1 (similar to mGlu5) is localized postsynaptically at perisynaptic/extrasynaptic sites (Lujan et al., 1996; Hepp et al., 2014). In addition, the behavioral and synaptic deficits that we observe in the GluD1 KO, including impaired NMDA receptor subunit switch and impaired pruning, are deficits observed in mouse models with mGlu5 dysfunction (Vanderklish and Edelman, 2002; Xu et al., 2009; Matta et al., 2011; Cruz-Martin et al., 2012). Moreover, a recent study demonstrated ion channel gating of GluD2 when coexpressed with mGlu1 (Ady et al., 2014). Based on this converging evidence, we hypothesized that GluD1 and mGlu5 are part of a common signaling complex, and that mGlu5 signaling will be impaired in GluD1 KO. Our results demonstrate that GluD1 and mGlu5 colocalize and coimmunoprecipitate in the hippocampus, and loss of GluD1 impairs Homer-mGlu5 interaction and the downstream mechanistic target of rapamycin (mTOR) signaling pathway. Additionally, a deficit in mGlu5-mediated  $\alpha$ -amino-3-hydroxy-5-methyl-4-isoxazolepropionic acid (AMPA) receptor internalization was found in GluD1 KO. Together, our data provide evidence for a novel role of GluD1 in the regulation of mGlu5 signaling in the hippocampus.

## Materials and Methods

### Animals

The GluD1 KO mice were obtained from Dr. Jian Zuo (St. Jude Children's Hospital, Memphis, TN) (Gao et al., 2007) and maintained as previously described (Yadav et al., 2012) at a constant temperature ( $22 \pm 1^\circ\text{C}$ ) and a 12-hour light-dark cycle with free access to food and water. Only male mice were used for these studies. In this study, strict measures were taken to minimize pain and suffering to animals in accordance with the recommendations in the Guide for Care and Use of Laboratory Animals of the National Institutes of Health. All experimental protocols were approved by the Creighton University Institutional Animal Care and Use Committee.

### Reagents

(*RS*)-3,5-dihydroxyphenylglycine (DHPG), (*RS*)-2-chloro-5-hydroxyphenylglycine (CHPG) (Abcam, Cambridge, UK), 2-methyl-6-(phenylethynyl)pyridine (MPEP), and DL-2-amino-5-phosphonopentanoic acid (DL-AP5) (Tocris Bioscience, Bristol, UK) were used in this study. Stock solutions were prepared with recommended solvents, either water (DHPG, CHPG), dimethylsulfoxide (MPEP), or equimolar NaOH (DL-AP5), and stored at  $-20^\circ\text{C}$ . Final concentrations for the *in vitro* treatment were prepared by diluting stock solutions with artificial cerebrospinal fluid (aCSF). Stock solutions for DHPG and CHPG were used within a week of preparation. The mGlu5 construct was provided by Dr. Shigetada Nakanishi (Osaka Bioscience Institute, Osaka, Japan), and the hemagglutinin-GluD1 (HA-GluD1) construct was a gift from Dr. Michisuke Yuzaki (Keio University, Tokyo, Japan).

### Immunohistochemistry

For immunohistochemistry, animals were anesthetized with isoflurane and transcardially perfused with ice-cold fixative containing 4% paraformaldehyde in 0.1 M phosphate buffer (PB, pH 7.4). After perfusion, brains were removed and immersed in the same fixative overnight at  $4^\circ\text{C}$ . Tissue blocks were washed thoroughly in 0.1 M PB (three times). Coronal 60- $\mu\text{m}$ -thick sections were cut on a Vibratome

(VT1000; Leica, Buffalo Grove, IL). Thereafter, sections were incubated in 10% normal goat serum (NGS) diluted in 50 mM Tris buffer (pH 7.4) containing 0.9% NaCl [Tris-buffered saline (TBS)], with 0.2% Triton X-100, for 1 hour. Subsequently, sections were incubated in anti-GluD1 antibody [gift from Dr. Ludovic Tricoire (Centre National de la Recherche Scientifique, Paris, France)] at 1:15,000 dilution in TBS containing 1% NGS overnight at  $4^\circ\text{C}$ . After washing three times (5 minutes each) with PB, sections were incubated with secondary antibody goat anti-rabbit Alexa Fluor 647 (1:500, diluted in TBS containing 1% NGS) (ThermoFisher Scientific, Waltham, MA) for 2 hours at room temperature. Finally, sections were mounted on a glass slide after washing (three times, 5 minutes each) with PB, and a coverslip was placed after adding Fluoromount-G (Southern Biotechnology Inc., Birmingham, AL). Images were obtained using a Leica TCS SP8 MP confocal microscope at  $1024 \times 1024$  pixels. A threshold was set for imaging based on minimal nonspecific staining in knockout sections.

For colabeling following GluD1 staining, the sections were blocked in 10% normal donkey serum (NDS) diluted in 50 mM Tris buffer (pH 7.4) containing 0.9% NaCl (TBS), with 0.2% Triton X-100, for 1 hour. Subsequently, sections were incubated in anti-mGlu5 antibody (1:1000 diluted in TBS containing 1% NDS; number AB5675; EMD Millipore, Temecula, CA) overnight at  $4^\circ\text{C}$ . After washing three times (5 minutes each) with PB, sections were incubated with secondary antibody donkey anti-rabbit Alexa Fluor 488 (1:500, diluted in TBS containing 1% NDS) for 2 hours at room temperature. Finally, sections were mounted on a glass slide after washing (three times, 5 minutes each) with PB, and a coverslip was placed after adding Fluoromount-G.

### Immunoprecipitation

**Immunoprecipitation of mGlu5 from Synaptosomal Membrane Fraction.** The synaptic plasma membrane fraction was prepared according to the procedure described previously (Blackstone et al., 1992). In brief, the hippocampus was dissected from mice at 4 weeks of age and homogenized in 10 volumes of buffer (0.32 M sucrose, 4 mM HEPES, pH 7.4). The homogenate was centrifuged (1000g for 10 minutes at  $4^\circ\text{C}$ ), and the resulting supernatant was again centrifuged (10,000g for 15 minutes at  $4^\circ\text{C}$ ). The pellet obtained from the aforementioned step was suspended in 10 volumes of HEPES-buffered sucrose and centrifuged (10,000g for 15 minutes at  $4^\circ\text{C}$ ) to yield the washed crude synaptosomal fraction. The resulting pellet was lysed by hypo-osmotic shock in 9 volumes of ice-cold water with protease/phosphatase inhibitors, and thereafter homogenized. The concentration of HEPES was adjusted rapidly to 4 mM, and the mixture was stirred constantly for 30 minutes at  $4^\circ\text{C}$  to ensure complete lysis. The lysate was centrifuged at 25,000g for 20 minutes at  $4^\circ\text{C}$ , and the resulting pellet was suspended in HEPES-buffered sucrose, layered onto a discontinuous sucrose gradient containing 0.8/1.0/1.2 M sucrose, and ultracentrifuged (150,000g for 2 hours at  $4^\circ\text{C}$ ). The fraction at the 1.0/1.2 M sucrose interface was isolated as the synaptic plasma membrane, and the protein concentration was determined. For immunoprecipitation, 100  $\mu\text{g}$  of protein was incubated with 2  $\mu\text{g}$  of mGlu5 antibody overnight at  $4^\circ\text{C}$ , followed by incubation with 30  $\mu\text{l}$  of protein A/G agarose bead slurry for 4 hours at  $4^\circ\text{C}$ . The beads were washed with phosphate-buffered saline (PBS). The resulting beads were boiled in Laemmli's buffer for 10 minutes, and the supernatant was used for immunoblot of mGlu5 and GluD1.

**Immunoprecipitation in Heterologous Expression System.** Human embryonic kidney 293 (HEK293) cells were maintained in 60-mm sterile dishes in Dulbecco's modified Eagle's medium ( $1\times$ ; containing 1 g/l D-glucose, L-glutamine, and 110 mg/l sodium pyruvate) supplemented with 10% fetal bovine serum and 1% penicillin streptomycin. HEK293 cells were transfected at 60–70% confluency using Lipofectamine 2000 (Invitrogen, Carlsbad, CA). Twenty microliters of Lipofectamine was used for transfection of a single 60-mm dish. Cells

were transfected with either 4.5  $\mu\text{g}$  of pCIneo GluD1 (Yadav et al., 2011) or pCAGGS HA-GluD1 (gift from Dr. M. Yuzaki) and 3.5  $\mu\text{g}$  of pCIneo mGlu5 (gift from Dr. S. Nakanishi). Cells were collected 40–48 hours after transfection for immunoprecipitation studies. In brief, the culture dish was kept on ice and gently washed with 0.1 M PBS. Thereafter, the cells were scraped and collected in 150  $\mu\text{l}$  of IP buffer (50 mM Tris, 120 mM NaCl, 1% NP40, pH 7.4) containing phosphatase inhibitor cocktail, protease inhibitor cocktail (Sigma-Aldrich, St. Louis, MO), and phenylmethylsulfonyl fluoride (PMSF) (10  $\mu\text{l}$  of each per 1 ml of IP buffer). The sample was subjected to three sonication pulses and centrifuged at 13,000g at 4°C for 10 minutes. The supernatant was collected and the protein concentration determined using the Bradford assay. Thereafter, immunoprecipitation and western blotting were performed. The protein was diluted to 1  $\mu\text{g}/\mu\text{l}$  in the IP buffer. Two hundred micrograms of protein was taken for each sample type, and primary antibody (1  $\mu\text{g}$  of antibody/100  $\mu\text{g}$  of protein) was added and incubated overnight at 4°C with gentle rocking. Thirty microliters of protein A-agarose bead slurry was added (50% in PBS) to the aforementioned mixture and incubated for 4 hours at 4°C with gentle rocking. The mix was then microcentrifuged for 60 seconds at 2000 rpm at 4°C. The pellet was washed twice with 100  $\mu\text{l}$  of 0.1 M PBS on ice. The pellet was resuspended in 20  $\mu\text{l}$  of Laemmli's buffer and boiled for 5 minutes, and western blotting was performed.

**Immunoprecipitation of Homer from Total Protein.** For these experiments, brain sections were first prepared. Wild-type and GluD1 KO animals (24–30 days old) were anesthetized using isoflurane, then decapitated. The brain was isolated and mounted on the Vibratome (Leica VT 1000S), and 300- $\mu\text{m}$  horizontal sections were obtained. The slice cutting solution consisted of 115 mM sucrose, 3.5 mM KCl, 24 mM  $\text{NaHCO}_3$ , 1.25 mM  $\text{NaH}_2\text{PO}_4$ , 10 mM glucose, 1 mM  $\text{CaCl}_2$ , and 3 mM  $\text{MgCl}_2$ . The procedures from brain isolation to Vibratome sectioning were performed under chilled conditions. After cutting, the sections were incubated in the aCSF, consisting of 122 mM NaCl, 3.5 mM KCl, 24 mM  $\text{NaHCO}_3$ , 1.25 mM  $\text{NaH}_2\text{PO}_4$ , 10 mM glucose, 2.4 mM  $\text{CaCl}_2$ , and 2.5 mM  $\text{MgCl}_2$  at 30°C for 1 hour and at room temperature thereafter, and used for experiments 2–3 hours after sectioning. The slices were placed on perforated inserts in a six-well plate. The slice cutting and incubation solutions were bubbled with 5%  $\text{CO}_2$  at all times.

Horizontal hippocampal slices were either vehicle-treated or treated with 100  $\mu\text{M}$  DHPG for 5 minutes (in the presence of 100  $\mu\text{M}$  DL-AP5). After treatment, the slices were washed twice with aCSF and were allowed to incubate for 60 minutes in the aCSF. After incubation, the cornu ammonis 1 (CA1) region of the hippocampus was dissected on ice under a dissecting microscope using fine dissection instruments or using a tissue punch. The tissue was thereafter homogenized in IP buffer [50 mM Tris, 120 mM NaCl (pH 7.4), 0.5% NP40]. To pull down Homer, the lysates were incubated overnight with Homer antibody (dilution 1:100; Santa Cruz Biotechnology, Dallas, TX) at 4°C with gentle rocking. Protein A/G agarose bead slurry (Thermo Fisher Scientific, Waltham, MA) was washed twice with IP buffer, added to the lysates, and incubated at 4°C for 4 hours. The beads were then washed with IP buffer two times and recollected by centrifugation at 3500g for 1 minute. The beads were boiled in Laemmli's buffer for 5 minutes, supernatant was collected after centrifugation at 3500g for 1 minute, and western blotting was performed.

### Western Blot Analysis

For estimation of protein kinase B (Akt), mTOR, and extracellular signal-regulated kinase (ERK) horizontal hippocampal sections were treated with vehicle or 100  $\mu\text{M}$  DHPG for 5 minutes (in the presence of 100  $\mu\text{M}$  DL-AP5). After the specified duration of incubation (0, 5, 15, and 60 minutes), slices were washed twice with aCSF under chilled conditions, and the CA1 region was dissected and immediately homogenized in RIPA buffer. The homogenates were sonicated (three pulses with 5-second intervals) and boiled in Laemmli's buffer for 5 minutes, and western blotting was performed. Rate of protein

translation was evaluated using a puromycin assay as previously described (Schmidt et al., 2009). In brief, after 2–3 hours of recovery, slices were incubated with puromycin antibiotic (5  $\mu\text{g}/\text{ml}$ ) in aCSF for 45 minutes. For mGlu1/5 activation, 100  $\mu\text{M}$  DHPG (in the presence of DL-AP5) was applied for the first 5 minutes together with puromycin, followed by incubation with aCSF with puromycin alone. Thereafter, slices were chilled on dry ice, and the CA1 region was microdissected. The protein from the CA1 region was extracted, and western blot was performed for puromycin. Specificity of puromycin assay was determined in wild-type slices, where basal puromycin incorporation was found to be sensitive to protein translation inhibitor cycloheximide, and no nonspecific labeling was observed when puromycin was absent.

Protein samples were resolved on SDS-PAGE gel and transferred onto a nitrocellulose membrane. Membranes were blocked with 5% bovine serum albumin or milk in Tris-buffered saline/Tween 20 at room temperature for 1 hour and incubated with appropriate antibodies overnight at 4°C [mTOR, phospho-mTOR, Akt, phospho-Akt, ERK1/2, and phospho-ERK1/2 were used at 1:1000 (Cell Signaling Technology, Danvers, MA); Homer, 1:1000 (Santa Cruz Biotechnology); mGlu5, 1:500 (EMD Millipore); GluA1 subunit and GluA2 subunit, 1:1000 (EMD Millipore); actin, 1:1000 (ABR Affinity Bioreagents, Golden, CO); puromycin, 1:2000 (EMD Millipore); HA, 1:1000 (Covance, Princeton, NJ); and GluD1, 1:1000 (Alomone Laboratories, Jerusalem, Israel)]. The blots were incubated in appropriate secondary antibody prepared in 5% milk solution at room temperature for 1 hour. Blots were developed using an enhanced chemiluminescent kit (GE Healthcare, Piscataway, NJ). Images were taken using Precision Illuminator Model B95 (Imaging Research Inc., St. Catharines, Canada) with an MTI CCD 72S camera (Michigan City, IN) and analyzed using MCID Basic software, version 7.0 (Imaging Research). For analysis of protein expression, the optical density of each sample was normalized with appropriate controls. Each western blot data point in each group was obtained from a separate animal.

### Assessment of Surface AMPA Receptor Subunits

Horizontal hippocampal slices from approximately 4-week-old animals were sham treated or treated with 100  $\mu\text{M}$  RS-DHPG (in the presence of 100  $\mu\text{M}$  DL-AP5) for 5 minutes. After treatment, the slices were washed three times with 5 ml of aCSF. For the specific mGlu5 and mTOR antagonist experiment, the slices were pretreated for 20 minutes with 10  $\mu\text{M}$  MPEP or 200 nM rapamycin, respectively. For the mGlu5-specific agonist experiment, the slices were treated with CHPG (300  $\mu\text{M}$  for 15 minutes). The slices were incubated for another 15 or 60 minutes before placing them on ice. The CA1 region of the hippocampus was dissected from the slices and incubated with N-hydroxysuccinimidobiotin biotin (1.5 mg/ml, made fresh immediately before use) for 1 hour on ice. After this step, to quench the biotinylation reaction, the slices were washed with 10 mM glycine solution in ice-cold aCSF and TBS for 5 minutes twice, followed by washing with aCSF for 5 minutes twice. The dissected slices were homogenized in RIPA buffer with 25 gauge needle. The homogenates were incubated over the ice for 10 minutes and sonicated with three pulses at 5-second intervals. Samples were centrifuged at 13,000g for 10 minutes, and supernatants were collected. Streptavidin beads were prewashed with binding buffer (0.1% SDS and 1% NP40 in 0.1 M PBS) and centrifuged at 3500g for 1 minute twice at 4°C to collect beads. For 3  $\mu\text{g}$  of protein, 2  $\mu\text{l}$  of reconstituted streptavidin bead slurry was used. A fraction of input samples was saved as total protein samples. From the remaining fraction, equal amounts of protein for each group were taken and diluted with RIPA buffer so that each sample would have an equal concentration (1  $\mu\text{g}/\mu\text{l}$ ). These samples were added to the streptavidin beads and incubated overnight at 4°C. After incubation, the beads were washed with binding buffer twice, and beads were collected by centrifugation at 3500g for 1 minute. The beads were boiled in Laemmli's buffer for 5 minutes. The samples were microcentrifuged at 3500g for 1 minute. The supernatant was collected (hereafter referred to as surface protein fraction), probed by western blotting,

and normalized to input samples, which are referred to as total protein.

## Results

### GluD1 Interacts with mGlu5 in the Hippocampus.

The general expression pattern of mGlu5 is very similar to that of GluD1, and at excitatory synapses, these two receptors appear to be located at the perisynaptic region (Lujan et al., 1996; Shigemoto and Mizuno, 2000; Hepp et al., 2014; Konno et al., 2014). These findings suggest possible direct or indirect interactions between mGlu5 and GluD1 proteins. To further investigate this interaction, we performed colabeling experiments using a GluD1-specific antibody. As seen in Fig. 1A, the puncta for GluD1 (red) overlapped with mGlu5 puncta (green) at several places, producing distinct yellow puncta. This result shows that mGlu5 and GluD1 are expressed at a close proximity to one another in the hippocampus. Absence of GluD1 staining in GluD1 KO tissue confirmed the antibody specificity (Supplemental Fig. 1A). Many of the puncta for GluD1 and mGlu5 also colocalized with PSD95 puncta, indicating that these are likely to be synaptic in nature (Supplemental Fig. 1B). To further verify protein interaction between GluD1 and mGlu5, we performed coimmunoprecipitation in wild-type samples from the hippocampus and striatum, since both GluD1 and mGlu5 are highly expressed

in these two regions. We found that GluD1 coimmunoprecipitated with mGlu5 in both the hippocampus and striatum (Fig. 1B; Supplemental Fig. 1D; experiments were repeated five times), demonstrating potential direct or indirect interactions between GluD1 and mGlu5 proteins. No immunoprecipitation was observed in GluD1 KO, demonstrating specificity of the pulldown (Fig. 1B). The absence of the GluD1 band in GluD1 KO tissue confirmed the specificity of the antibody in western blotting (Supplemental Fig. 1C).

We further tested whether GluD1 and mGlu5 may interact with each other by expressing these proteins in HEK293 cells. We used an HA-tagged GluD1 construct. As indicated in Fig. 1C, we performed pulldown for mGlu5 followed by western blotting for mGlu5, GluD1, and HA. We found that pulldown of mGlu5 from protein lysate of cells transfected with mGlu5 and HA-GluD1 showed HA and GluD1 immunoreactivity, indicating that mGlu5 and GluD1 coimmunoprecipitate. The specificity of these results was confirmed by transfecting cells with mGlu5 and HA-GluD1 and performing reciprocal immunoprecipitation of HA (HA-GluD1), which leads to pulldown of mGlu5. We also performed pulldown of mGlu5 from cells transfected with mGlu5 and GluD1 constructs (data not shown). This resulted in pulldown of GluD1, further confirming results from the use of HA-tagged GluD1 construct. It should be noted that we do not fully understand whether GluD1 and mGlu5 exhibit direct interaction, since endogenous

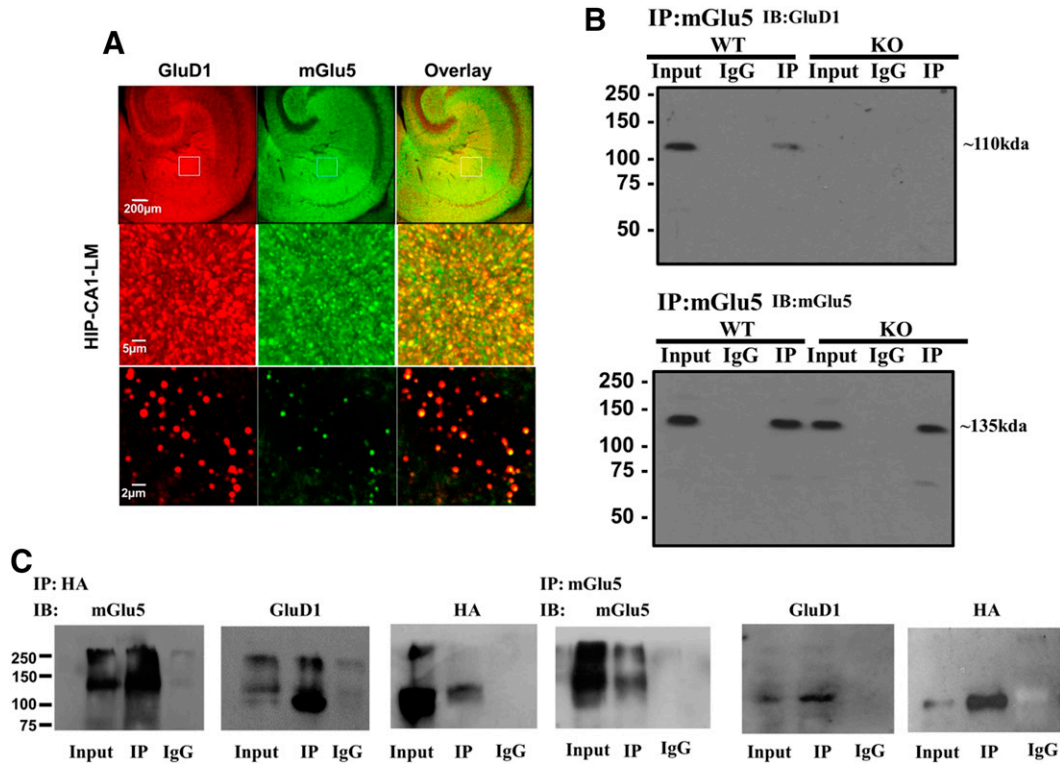


**Fig. 1.** mGlu5 and GluD1 colocalize and coimmunoprecipitate in the hippocampus (HIP). (A) Colabeling with GluD1 and mGlu5 was performed in fixed wild-type (WT) hippocampal sections. Confocal imaging demonstrates colocalization of GluD1 (red) and mGlu5 (green) punctas as indicated by yellow colabeling. CA1-LM, stratum lacunosum moleculare field of CA1. (B) Coimmunoprecipitation studies were performed where mGlu5 was immunoprecipitated from hippocampal synaptosomal membrane fraction preparation, followed by western blotting for GluD1 and mGlu5. GluD1 protein was found to immunoprecipitate with mGlu5 protein. Experiments were repeated five times with protein collected from separate animals, and similar results were obtained. No GluD1 pulldown was observed in GluD1 KO tissue and when IgG alone was used, demonstrating specificity of immunoprecipitation. (C) mGlu5 and GluD1 interaction was tested in HEK293 cells. Cells were transfected with mGlu5 and HA-GluD1, and pulldown of mGlu5 or HA was performed from the protein lysate. GluD1 was found to coimmunoprecipitate with mGlu5. In addition, immunoprecipitation of HA (HA-GluD1) resulted in pulldown of mGlu5. The experiment was repeated five times with similar results. IB, immunoblot.

proteins in HEK cells may coordinate an interaction between GluD1 and mGlu5. Further experiments are required to address this question.

**Disruption of mGlu5-Homer Interactions in GluD1 KO.** In light of the potential interaction between GluD1 and mGlu5, it is conceivable that loss of GluD1 may affect the scaffolding interactions of mGlu5 if GluD1 serves as a mediator of these interactions or helps stabilize these interactions. It is well known that mGlu5 interacts with long isoforms of Homer (Homer 1b, 1c, 2, and 3), and the mGlu5-Homer interaction is critical for downstream mTOR signaling (Kato et al., 1998; Tu et al., 1999; Ronesi and Huber, 2008; Ronesi et al., 2012). Using immunoprecipitation and western blotting, we assessed whether loss of GluD1 affects the mGlu5-Homer coupling. We first confirmed that loss of GluD1 did not affect the basal expression of mGlu5 (Fig. 2A). We next assessed Homer and mGlu5 interaction under basal conditions and after mGlu5/5 activation by DHPG (5-minute followed by 60-minute incubation) by performing pull-down for Homer from microdissected CA1 hippocampal tissue followed by western blotting for mGlu5. Degree of association was plotted as a ratio of optical density for mGlu5 over Homer, and all values were normalized to the average of the basal wild-type ratio (Fig. 2B). Two-way analysis of variance (ANOVA) revealed a significant interaction effect ( $P < 0.001$ ) as well as genotype ( $P < 0.01$ ) and treatment ( $P < 0.05$ ) effects in the mGlu5-Homer interaction. Further comparison between wild type and GluD1 KO under basal condition revealed a significantly lower mGlu5-Homer interaction in GluD1 KO ( $P < 0.05$ , unpaired  $t$  test; Fig. 2B). Such lower interaction is also observed in FMR1 knockout and is proposed to lead to constitutive activation of mGlu5 (Ronesi et al., 2012). We also found that the mGlu5-Homer interaction was reduced in wild-type animals after DHPG treatment ( $P < 0.05$ , unpaired  $t$  test). This is in accordance with sequestration of mGlu5/5 by Homer1a, which is translated locally in an activity-driven manner after DHPG treatment, thereby reducing the interaction of the long forms of Homer with mGlu5/5 (Kammermeier

et al., 2000; Kammermeier and Worley, 2007). However, it should be noted that others have reported an increase in mGlu5-Homer interaction after DHPG treatment (Rong et al., 2003; Hu et al., 2012). These differences may be attributable to the use of a different model system and duration of mGlu5 agonist exposure. In GluD1 KO mice, we found that the interaction between the long Homer isoforms and mGlu5 is enhanced after DHPG treatment ( $P < 0.01$ ; Fig. 2B). This finding may be explained by potential disruption of normal activity-dependent modulation of mGlu5 scaffold in GluD1 KO (Gupta et al., 2015). For example, loss of GluD1 may impair upregulation of the short-form Homer in response to mGlu5 activation, which may thereby prevent the sequestration of mGlu5.

**Loss of GluD1 Leads to Basally Overactive mGlu5-Mediated Akt-mTOR Signaling in the Hippocampus.** The mGlu5-Homer interaction is known to regulate the downstream mTOR signaling (Ronesi et al., 2012). Activation of mTOR complexes, mTORC1 and mTORC2, downstream of mGlu5 activation leads to protein translation and actin reorganization, respectively, and is critical for functional and structural plasticity. We tested whether dysregulation of mGlu5-Homer interaction in GluD1 KO impacted the downstream mTOR signaling both under basal conditions and in response to mGlu5/5 agonist DHPG. We found that the basal levels of active mTOR and Akt (Ser2481 phospho-mTOR and Ser473 phospho-Akt) were higher in microdissected CA1 regions of the hippocampus in GluD1 KO ( $P < 0.01$ , unpaired  $t$  test; Fig. 3A). Similar higher basally active mTOR and Akt were also observed in GluD1 KO in hippocampal synaptoneuroosomes obtained from acutely dissected hippocampus, showing that these results were independent of sample preparation or brain slicing (data not shown). Furthermore, DHPG (100  $\mu$ M for 5 minutes) was found to produce an increase in mTOR and Akt activation similar to previous reports (Hou and Klann, 2004; Ronesi and Huber, 2008) ( $P < 0.05$ , one-way ANOVA). However, this increase in mTOR and Akt activation was absent in GluD1 KO (Fig. 3A),

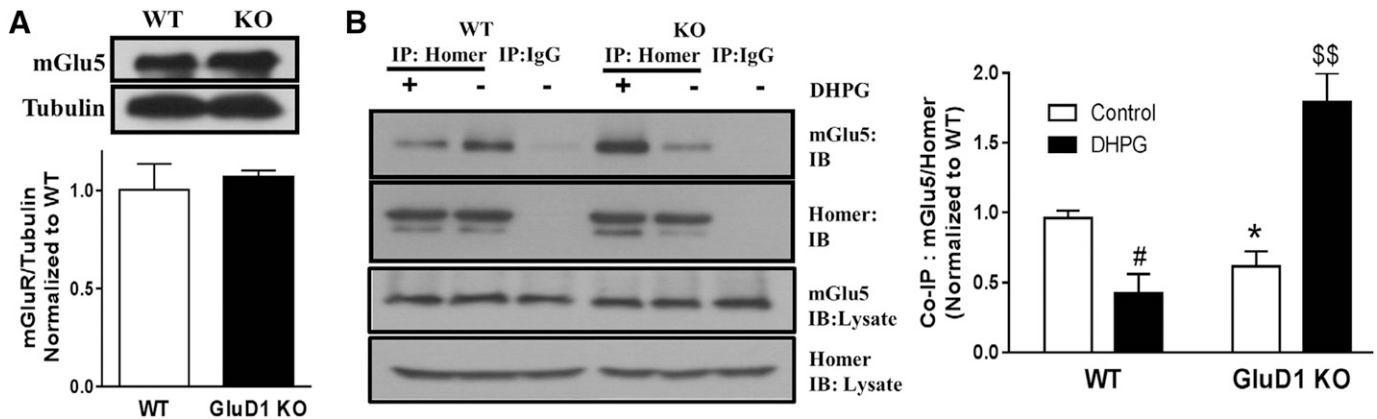


**Fig. 2.** Reduced basal interaction of mGlu5 with the long isoform of Homer due to loss of GluD1. (A) GluD1 KO does not exhibit a detectable change in mGlu5 expression in total protein fraction from the CA1 region ( $N = 5$ ). (B) Degree of interaction between mGlu5 and Homer was assessed in wild-type (WT) and GluD1 KO under basal conditions and in response to DHPG. Horizontal hippocampal sections were either sham treated with aCSF or treated with DHPG (100  $\mu$ M, 5 minutes) followed by collection of total protein after 60 minutes. Immunoprecipitation was performed for Homer (long isoform) followed by immunoblotting for mGlu5 and Homer. Under basal conditions, the ratio of mGlu5/Homer was lower in GluD1 KO ( $*P < 0.05$ , unpaired  $t$  test). Treatment with DHPG reduced the interaction between mGlu5 and Homer in wild-type CA1 ( $\#P < 0.05$ ) but produced an increase in interaction in GluD1 KO ( $$$P < 0.01$ ). Amount of mGlu5 and Homer in the total lysate used for immunoprecipitation was unaltered between wild-type and GluD1 KO or by treatment.  $N = 3$  mice/genotype. The optical density was normalized to control value for individual experiments. Additionally, the individual control values were normalized to average of control. IB, immunoblot.

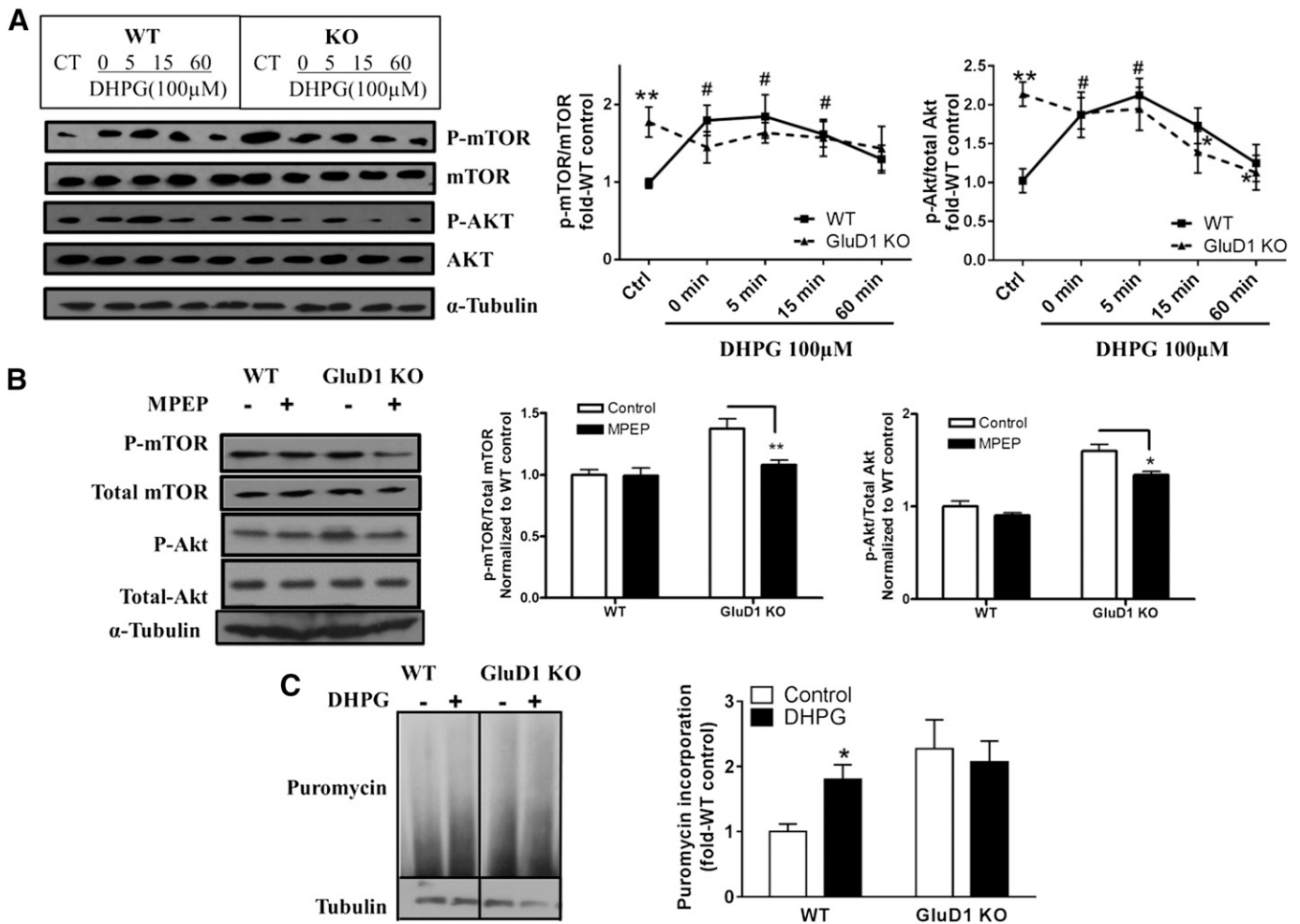


**Fig. 3.** Elevated basal levels of phospho-Akt (p-Akt) and phospho-mTOR (p-mTOR) and lack of DHPG-induced p-Akt and p-mTOR increase in GluD1 KO. (A) Total protein from CA1 region of hippocampal horizontal sections was collected either with aCSF control treatment or after treatment with DHPG (100  $\mu$ M, 5 minutes) for various times. Higher basal levels of p-mTOR (Ser2481) and p-Akt (Ser473) were observed in GluD1 KO (\*\* $P$  < 0.01, unpaired  $t$  test). An increase in p-mTOR and p-Akt levels was observed in the CA1 region in wild-type (WT) mice from 0 to 5 minutes after treatment with DHPG (# $P$  < 0.05 compared with wild-type control, one-way ANOVA), but this increase was absent in GluD1 KO ( $N$  = 5–8 for each group). (B) Pretreatment with mGlu5-specific inhibitor MPEP (10  $\mu$ M for 20 minutes) reduced the elevated p-mTOR and p-Akt levels in the GluD1 KO CA1 region ( $N$  = 4; \* $P$  < 0.05, \*\* $P$  < 0.01 compared with GluD1 KO control, unpaired  $t$  test). (C) A significant genotype effect was observed in the puromycin incorporation assay to detect protein translation ( $N$  = 6;  $P$  < 0.05, two-way ANOVA). In addition, a significant increase in puromycin incorporation was observed with DHPG in wild-type slices (\* $P$  < 0.05, unpaired  $t$  test); however, this effect of DHPG was absent in GluD1 KO slices. CT, control.

suggesting potential occlusion or saturation of this pathway. No difference in the basal phospho-ERK level was observed, indicating specificity of this effect for the Akt-mTOR pathway (data not shown). Using a pharmacological approach, we further addressed whether enhanced mGlu5 signaling underlies the upregulation in the Akt-mTOR pathway. We found that the higher basal levels of phospho-mTOR ( $P$  < 0.01) and phospho-Akt ( $P$  < 0.05) in GluD1 KO CA1 were significantly reduced with selective mGlu5 antagonist MPEP (Fig. 3B), suggesting that overactive mGlu5 signaling at least partly underlies the higher Akt-mTOR pathway. The mTORC1 pathway mediates protein translation, which initiates synaptic plasticity and long-term depression upon mGlu1/5 activation. Thus, we further tested whether basal and DHPG-induced rate of protein translation is altered in GluD1 KO using the puromycin incorporation assay. Two-way ANOVA revealed a significant genotype effect in puromycin incorporation ( $P$  < 0.05). In agreement with an increase in protein translation in response to mGlu1/5 activation, we observed

higher puromycin incorporation in wild-type slices treated with DHPG ( $P$  < 0.05, unpaired  $t$  test; Fig. 3C); however, DHPG-induced increase in puromycin incorporation was absent in GluD1 KO slices. Together, these findings demonstrate that loss of GluD1 leads to basally upregulated mGlu5-mediated Akt-mTOR signaling, which potentially saturates and impairs further activation in response to mGlu1/5 agonist DHPG and impacts protein translation.

**Abnormal mGlu5-Mediated AMPA Receptor Internalization Due to Loss of GluD1.** Activation of mGlu5 leads to a protein-translation-dependent increase in mediators involved in AMPA receptor endocytosis (Snyder et al., 2001; Bear et al., 2004). Since mGlu5-mediated protein synthesis was abolished by GluD1 deletion, we investigated whether mGlu5-mediated AMPA receptor internalization was also affected in GluD1 KO. Using surface biotinylation as an assay, we quantitatively tested whether endocytosis of surface AMPA receptor subunit GluA1 is affected in GluD1 KO. We measured the surface and total GluA1 expression in wild-type,

GluD1 heterozygous, and GluD1 KO CA1 hippocampus in response to DHPG. Two-way ANOVA analysis of the ratio of surface to total GluA1 expression revealed a significant interaction ( $P < 0.01$ ) and genotype effect ( $P < 0.001$ ) in the level of GluA1 subunit internalization. Furthermore, we found that DHPG (100  $\mu\text{M}$ ) caused a significant reduction in surface GluA1 in CA1 hippocampus from wild-type mice ( $P < 0.01$ , one-way ANOVA) in accordance with a role of mGlu1/5 in synaptic depression. However, this reduction in GluA1 surface expression was absent in GluD1 KO mice, and in fact, an opposite trend was observed ( $P < 0.05$ , one-way ANOVA; Fig. 4A). Similar impairment in internalization of the GluA2 subunit of AMPA receptors was also observed in GluD1 KO (data not shown). Moreover, internalization of GluA1 was absent in slices prepared from GluD1 heterozygous animals, demonstrating that lower expression of GluD1 is sufficient to impair DHPG-induced AMPA receptor internalization (Fig. 4A). Additional experiments using mGlu5-specific inhibitor (MPEP) and agonist (CHPG) demonstrated that the effects of AMPA receptor internalization were specific to mGlu5 activation. Specifically, internalization of GluA1 by DHPG was blocked in wild-type slices in the presence of MPEP (Fig. 4B). Furthermore, the mGlu5-selective agonist CHPG produced internalization in wild-type slices ( $P < 0.05$ ) but not in GluD1

KO slices (Fig. 4C). Such aberrant synaptic plasticity mechanisms may explain some of the learning and memory deficits in GluD1 KO, especially a deficit in hippocampus-dependent reversal learning of a spatial memory task (Yadav et al., 2013).

### Discussion

Recent studies demonstrate that GluD1 is enriched in the forebrain as well as the cerebellum during both early development and adulthood (Hepp et al., 2014; Konno et al., 2014). GluD1 is particularly abundant in the hippocampus, with high mRNA and protein expression in pyramidal neurons (Hepp et al., 2014). In addition, electron microscopy analysis demonstrates that GluD1 is located postsynaptically at excitatory synapses in the hippocampus (Hepp et al., 2014). We have recently identified a critical role of GluD1 in the development of excitatory synapses in the hippocampus as well as the prefrontal cortex. Specifically, loss of GluD1 prevents the normal developmental pruning of dendritic spines and leads to a higher number of excitatory synapses in adulthood (Gupta et al., 2015). Loss of GluD1 also impairs the normal switch from GluN2B to GluN2A NMDA receptor subunit in the hippocampus and cortex (Gupta et al., 2015). Here, we report that GluD1 colocalizes and interacts with the mGlu5 receptor

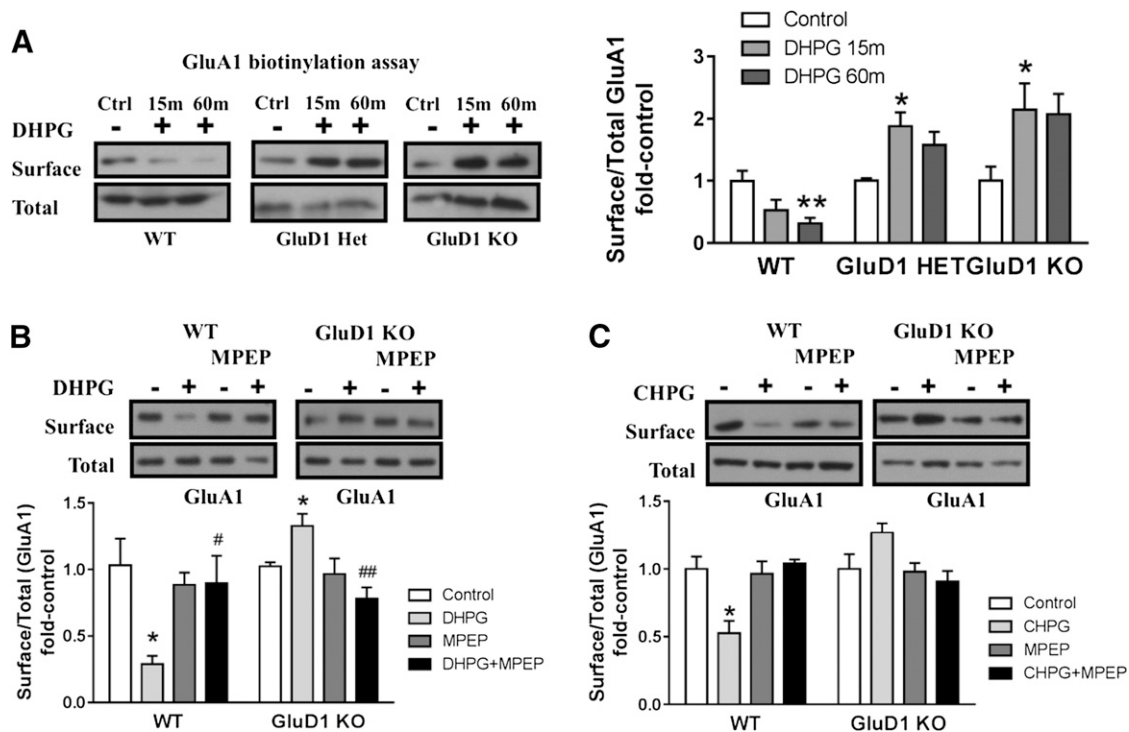


**Fig. 4.** GluD1 deletion leads to abnormal mGlu5-mediated AMPA receptor internalization in acute hippocampal slices. (A) Biotinylation assays to detect changes in surface expression of GluA1 were performed in horizontal sections from wild-type (WT), GluD1 heterozygous, and GluD1 KO mice. DHPG (100  $\mu\text{M}$ , 5 minutes in the presence of NMDA receptor antagonist) produced a reduction in surface GluA1 expression in wild-type sections ( $**P < 0.01$ , one-way ANOVA;  $N = 6-8$  for each data point). In GluD1 KO, no reduction in the surface expression was observed, whereas a contrasting increase in surface GluA1 expression was observed after 15 minutes of DHPG treatment ( $*P < 0.05$ , one-way ANOVA;  $N = 7-9$ ). Impaired internalization of surface GluA1 was also observed in GluD1 heterozygous mice ( $*P < 0.05$ , one-way ANOVA;  $N = 3$ ). (B) DHPG treatment induced significant reduction in surface GluA1 in slices prepared from the wild type ( $*P < 0.05$ , unpaired  $t$  test compared with respective control) and an opposing increase in surface GluA1 expression in GluD1 KO animals ( $*P < 0.05$ , unpaired  $t$  test compared with respective control). Pretreatment with mGlu5-specific antagonist MPEP inhibited GluA1 internalization in wild-type slices, indicating the requirement of mGlu5 in this effect ( $N = 4-5$ ). A significant difference was also observed between DHPG and DHPG+MPEP in wild-type as well as GluD1 KO ( $\#P < 0.05$  and  $\#\#P < 0.01$ , unpaired  $t$  test), supporting the requirement of mGlu5 in the effects produced by DHPG. (C) mGlu5-selective agonist CHPG leads to internalization of GluA1 in wild-type slices ( $*P < 0.05$ , unpaired  $t$  test), which was blocked by MPEP treatment. However, CHPG application failed to induce GluA1 internalization in GluD1 KO ( $N = 3$ ). In each case, treatment groups were normalized to sham control of the respective genotype. Ctrl, control; Het, heterozygous.

in the hippocampus and striatum, regions where abundant expression of these receptors is observed (Shigemoto and Mizuno, 2000; Konno et al., 2014). Moreover, the mGlu5 interaction with scaffold protein Homer and downstream Akt-mTOR pathway is dysregulated in the absence of GluD1. An interaction between delta receptors and mGlu5 has precedence from previous studies. In particular, studies indicate a reciprocal interaction between GluD2 and mGlu1 receptors in the cerebellar Purkinje cells. GluD2 physically associates with mGlu1, PLC $\gamma$ , and TRPC3 channels in Purkinje cells and regulates mGlu1 function (Uemura et al., 2004; Kato et al., 2012), whereas activation of mGlu1 appears to induce gating of GluD2 (Ady et al., 2014). Our data demonstrate that this interaction may extend to GluD1 and mGlu5 in the forebrain, which may serve as a mechanism to regulate excitatory synapses.

The G $_q$ -coupled mGlu5 is highly expressed at excitatory synapses in the CA1 hippocampal neurons (Lujan et al., 1996) and contributes to a number of postsynaptic functions in the central nervous system, such as increased neuronal excitability, intracellular Ca $^{2+}$  increase, synaptic plasticity, and pain (Snyder et al., 2001; Ireland and Abraham, 2002; Gubellini et al., 2003; Rae and Irving, 2004). Homer proteins are known to link mGluRs to other postsynaptic density proteins (Shiraishi-Yamaguchi and Furuichi, 2007; Niswender and Conn, 2010) and play a vital role in coupling the receptors with downstream effectors (Mao et al., 2005; Jung et al., 2007; Won et al., 2009). Disrupted interaction between mGlu5 and the long isoform of Homer leads to deficits in mTOR signaling, protein translation, as well as synaptic plasticity in the FMR1 knockout mouse model (Ronesi and Huber, 2008; Ronesi et al., 2012). We found that the Akt-mTOR phosphorylation was increased under basal conditions in the GluD1 KO. In addition, we found that MPEP reduced these basally higher levels, and both the Akt-mTOR pathway and protein translation were saturated and did not respond to DHPG (Fig. 5). The basally overactive mGlu5 signaling may be explained by a disruption in the normal conformation and interaction of mGlu5 with scaffolding proteins in the absence of GluD1. Alternatively, the increase in glutamatergic neurotransmission in GluD1 KO (Gupta et al., 2015) may lead to basally higher activation of mGlu5. These two mechanisms can also independently explain the impaired mGlu5 and long-form Homer interaction in GluD1 KO. Specifically, loss of GluD1 may directly affect mGlu5 interaction with long-form Homer, or Homer1a may be upregulated due to higher synaptic activity and then sequester mGlu5 and reduce interaction between mGlu5 and long-form Homer. Since a shift toward greater mGlu5 and Homer1a interaction favors constitutive activity of mGlu5 (Ango et al., 2001), this may explain the upregulated Akt-mTOR signaling in GluD1 KO. Further studies are needed to discriminate the precise mechanism underlying the upregulated mGlu5 signaling due to loss of GluD1.

**Phenotype Arising Due to Deletion of GluD1 and Relevance to Neurodevelopmental Disorders.** We found a deficit in early developmental processes, including dendritic spine pruning and switch in NMDA receptor subunit in GluD1 KO mice (Gupta et al., 2015). In addition, we previously demonstrated that GluD1 KO exhibits social-interaction and reversal-learning deficits and repetitive behaviors which are core features in several neurodevelopmental disorders, in

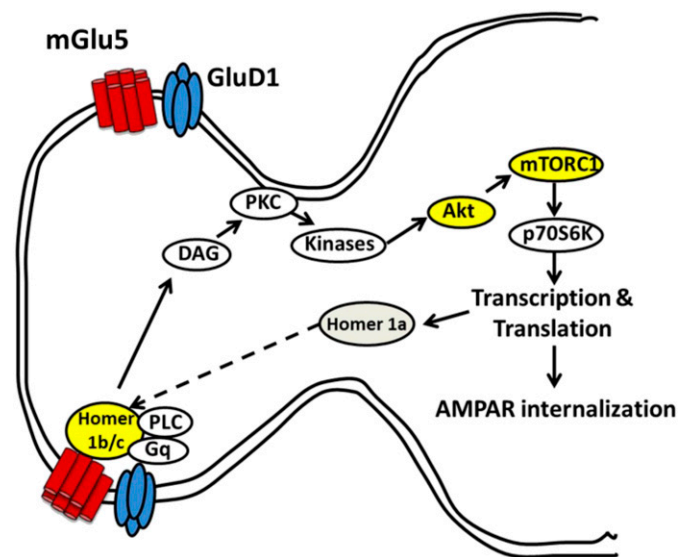


**Fig. 5.** Schematic representation of interaction between GluD1 and mGlu5 in the hippocampus. Our results demonstrate that GluD1 and mGlu5 colocalize at hippocampal synapses, and loss of GluD1 leads to a higher basal mGlu5-mediated Akt-mTOR signaling and impaired mGlu5 interaction with long-form Homer as well as a deficit in AMPA receptor (AMPA) internalization. DAG, diacylglycerol; PKC, protein kinase C; PLC, phospholipase C.

particular autism spectrum disorders (ASDs) (Yadav et al., 2012, 2013; Gupta et al., 2015). A recent study demonstrated that neurons derived from induced pluripotent stem cells from Rett syndrome patients exhibit an upregulation of GluD1 (Livede et al., 2015). Mutations in the methyl CpG binding protein 2 (MeCP2) gene, which leads to loss of function and/or expression of MeCP2 protein, are the primary cause of Rett syndrome (Amir et al., 1999). Additionally, mutations in cyclin-dependent kinase-like 5 (Cdkl5) also produce Rett-like syndrome. The neuropathologies in the MeCP2 KO model of Rett syndrome include a reduction in dendritic spine density, lower glutamatergic synapses, and a shift in excitatory-inhibitory balance toward greater inhibition (Dani et al., 2005; Nelson et al., 2006; Chao et al., 2007; Blackman et al., 2012; Na et al., 2013). Reduction in spine density is also observed in brains from Rett syndrome patients (Chapleau et al., 2009). The majority of these features in animal models are reproduced in patients with MeCP2 mutation-derived neurons using the induced pluripotent stem cells (Marchetto et al., 2010). Moreover, using induced pluripotent stem cells, another research group identified that patient-derived neurons that carried mutations in MeCP2 and cyclin-dependent kinase-like 5 exhibit a common upregulation of GluD1 subunit expression (Livede et al., 2015). In addition, they found that MeCP2 binds to the promoter of the GRID1 gene that codes for GluD1 and may therefore regulate its expression. Interestingly, several synaptic phenotypes in MeCP2 KO and patient-derived neurons are in stark contrast to those we have found in GluD1 KO; specifically, GluD1 KO exhibit higher dendritic spine density, higher number of excitatory synapses, and higher excitatory neurotransmission (Gupta et al., 2015). In addition, behavioral phenotypes, such as hyperactivity, lower anxiety-like behavior, and enhanced working memory, observed in GluD1 KO mice (Yadav et al., 2012, 2013) also partly contrast to behaviors previously reported in the MeCP2 KO



model (Calfa et al., 2011; Guy et al., 2011; Castro et al., 2014). In this study, we found that GluD1 KO have upregulated Akt-mTOR signaling (Fig. 1), which is in contrast to the lower Akt-mTOR pathway activation in MeCP2 KO (Ricciardi et al., 2011). Thus, MeCP2 KO and GluD1 KO appear to be on the opposite ends of the neurodevelopmental disorder spectrum, supporting the hypothesis that upregulation of GluD1 in Rett syndrome may partly underlie the synaptic and behavioral phenotypes.

Our present studies are also relevant to the mGluR hypothesis of autism, which proposes that dysregulation of mGluR function is a critical neuropathology in ASDs (Bear et al., 2004). Abnormalities in mGlu5 signaling in the hippocampus have been reported in several models of ASDs, in particular the FMR1 KO model and mGlu5 antagonist reverse molecular and behavioral deficits in FMR1 knockout mice, and have also been tested in clinical trials for fragile-X patients, with some promising results (Dölen et al., 2007, 2010; Jacquemont et al., 2011). Our data demonstrate that GluD1 is an important regulator of mGlu5 signaling and protein synthesis, and further analysis of the roles of GluD1 is necessary to fully understand its contribution to central nervous system physiology and neuropsychiatric disorders.

#### Authorship Contributions

*Participated in research design:* Suryavanshi, Gupta, Yadav, Keshewani, Liu, Dravid.

*Conducted experiments:* Suryavanshi, Gupta, Yadav, Keshewani, Liu.

*Performed data analysis:* Suryavanshi, Gupta, Yadav, Keshewani, Liu, Dravid.

*Wrote or contributed to the writing of the manuscript:* Suryavanshi, Gupta, Yadav, Keshewani, Liu, Dravid.

#### References

- Ady V, Perroy J, Tricoire L, Piochon C, Dadak S, Chen X, Dusart I, Fagni L, Lamboloz B, and Levenes C (2014) Type 1 metabotropic glutamate receptors (mGlu1) trigger the gating of GluD2 delta glutamate receptors. *EMBO Rep* **15**:103–109.
- Amir RE, Van den Veyver IB, Wan M, Tran CQ, Francke U, and Zoghbi HY (1999) Rett syndrome is caused by mutations in X-linked MECP2, encoding methyl-CpG-binding protein 2. *Nat Genet* **23**:185–188.
- Ango F, Prézeau L, Muller T, Tu JC, Xiao B, Worley PF, Pin JP, Bockaert J, and Fagni L (2001) Agonist-independent activation of metabotropic glutamate receptors by the intracellular protein Homer. *Nature* **411**:962–965.
- Bear MF, Huber KM, and Warren ST (2004) The mGluR theory of fragile X mental retardation. *Trends Neurosci* **27**:370–377.
- Blackman MP, Djukic B, Nelson SB, and Turrigiano GG (2012) A critical and cell-autonomous role for MeCP2 in synaptic scaling up. *J Neurosci* **32**:13529–13536.
- Blackstone CD, Moss SJ, Martin LJ, Levey AI, Price DL, and Haganir RL (1992) Biochemical characterization and localization of a non-N-methyl-D-aspartate glutamate receptor in rat brain. *J Neurochem* **58**:1118–1126.
- Calfa G, Percy AK, and Pozzo-Miller L (2011) Experimental models of Rett syndrome based on MeCP2 dysfunction. *Exp Biol Med (Maywood)* **236**:3–19.
- Castro J, Garcia RI, Kwok S, Banerjee A, Petravic J, Woodson J, Mellios N, Tropea D, and Sur M (2014) Functional recovery with recombinant human IGF1 treatment in a mouse model of Rett Syndrome. *Proc Natl Acad Sci USA* **111**:9941–9946.
- Chao HT, Zoghbi HY, and Rosenmund C (2007) MeCP2 controls excitatory synaptic strength by regulating glutamatergic synapse number. *Neuron* **56**:58–65.
- Chapleau CA, Calfa GD, Lane MC, Albertson AJ, Larimore JL, Kudo S, Armstrong DL, Percy AK, and Pozzo-Miller L (2009) Dendritic spine pathologies in hippocampal pyramidal neurons from Rett syndrome brain and after expression of Rett-associated MECP2 mutations. *Neurobiol Dis* **35**:219–233.
- Cruz-Martín A, Crespo M, and Portera-Cailliau C (2012) Glutamate induces the elongation of early dendritic protrusions via mGluRs in wild type mice, but not in fragile X mice. *PLoS One* **7**:e32446.
- Dani VS, Chang Q, Maffei A, Turrigiano GG, Jaenisch R, and Nelson SB (2005) Reduced cortical activity due to a shift in the balance between excitation and inhibition in a mouse model of Rett syndrome. *Proc Natl Acad Sci USA* **102**:12560–12565.
- Dölen G, Carpenter RL, Ocain TD, and Bear MF (2010) Mechanism-based approaches to treating fragile X. *Pharmacol Ther* **127**:78–93.
- Dölen G, Osterweil E, Rao BS, Smith GB, Auerbach BD, Chattarji S, and Bear MF (2007) Correction of fragile X syndrome in mice. *Neuron* **56**:955–962.
- Edwards AC, Aliev F, Bierut LJ, Bucholz KK, Edenberg H, Hesselbrock V, Kramer J, Kuperman S, Nurnberger JI, Jr, and Schuckit MA et al. (2012) Genome-wide association study of comorbid depressive syndrome and alcohol dependence. *Psychiatr Genet* **22**:31–41.
- Fallin MD, Lasseur VK, Avramopoulos D, Nicodemus KK, Wolyniec PS, McGrath JA, Steel G, Nestadt G, Liang KY, and Haganir RL et al. (2005) Bipolar I disorder and schizophrenia: a 440-single-nucleotide polymorphism screen of 64 candidate genes among Ashkenazi Jewish case-parent trios. *Am J Hum Genet* **77**:918–936.
- Gao J, Maison SF, Wu X, Hirose K, Jones SM, Bayazitov I, Tian Y, Mittleman G, Matthews DB, and Zakharenko SS et al. (2007) Orphan glutamate receptor delta1 subunit required for high-frequency hearing. *Mol Cell Biol* **27**:4500–4512.
- Glessner JT, Wang K, Cai G, Korvatska O, Kim CE, Wood S, Zhang H, Estes A, Brune CW, and Bradfield JP et al. (2009) Autism genome-wide copy number variation reveals ubiquitin and neuronal genes. *Nature* **459**:569–573.
- Greenwood TA, Lazzaroni LC, Murray SS, Cadenhead KS, Calkins ME, Dobie DJ, Green MF, Gur RE, Gur RC, and Hardiman G et al. (2011) Analysis of 94 candidate genes and 12 endophenotypes for schizophrenia in the Consortium on the Genetics of Schizophrenia. *Am J Psychiatry* **168**:930–946.
- Griswold AJ, Ma D, Cukier HN, Nations LD, Schmidt MA, Chung RH, Jaworski JM, Salyakina D, Konidari I, and Whitehead PL et al. (2012) Evaluation of copy number variations reveals novel candidate genes in autism spectrum disorder-associated pathways. *Hum Mol Genet* **21**:3513–3523.
- Grossman AW, Elisseou NM, McKinney BC, and Greenough WT (2006) Hippocampal pyramidal cells in adult Fmr1 knockout mice exhibit an immature-appearing profile of dendritic spines. *Brain Res* **1084**:158–164.
- Gubellini P, Saulle E, Centonze D, Costa C, Tropepi D, Bernardi G, Conquet F, and Calabresi P (2003) Corticostriatal LTP requires combined mGluR1 and mGluR5 activation. *Neuropharmacology* **44**:8–16.
- Gupta SC, Yadav R, Pavuluri R, Morley BJ, Stairs DJ, and Dravid SM (2015) Essential role of GluD1 in dendritic spine development and GluN2B to GluN2A NMDAR subunit switch in the cortex and hippocampus reveals ability of GluN2B inhibition in correcting hyperconnectivity. *Neuropharmacology* **93**:274–284.
- Guy J, Cheval H, Selfridge J, and Bird A (2011) The role of MeCP2 in the brain. *Annu Rev Cell Dev Biol* **27**:631–652.
- Hepp R, Audrey Hay Y, Aguado C, Lujan R, Dauphinot L, Potier MC, Nomura S, Poirel O, El Mestikawy S, and Lamboloz B et al. (2015) Glutamate receptors of the delta family are widely expressed in the adult brain. *Brain Struct Funct* **220**:2797–2815.
- Hou L and Klann E (2004) Activation of the phosphoinositide 3-kinase-Akt-mammalian target of rapamycin signaling pathway is required for metabotropic glutamate receptor-dependent long-term depression. *J Neurosci* **24**:6352–6361.
- Hu JH, Yang L, Kammermeier PJ, Moore CG, Brakeman PR, Tu J, Yu S, Petralia RS, Li Z, and Zhang PW et al. (2012) Preso1 dynamically regulates group I metabotropic glutamate receptors. *Nat Neurosci* **15**:836–844.
- Ireland DR and Abraham WC (2002) Group I mGluRs increase excitability of hippocampal CA1 pyramidal neurons by a PLC-independent mechanism. *J Neurophysiol* **88**:107–116.
- Jacquemont S, Curie A, des Portes V, Torrioli MG, Berry-Kravis E, Hagerman RJ, Ramos FJ, Cornish K, He Y, and Paulding C et al. (2011) Epigenetic modification of the FMR1 gene in fragile X syndrome is associated with differential response to the mGluR5 antagonist AFQ056. *Sci Transl Med* **3**:64ra1.
- Jung KM, Astarita G, Zhu C, Wallace M, Mackie K, and Piomelli D (2007) A key role for diacylglycerol lipase-alpha in metabotropic glutamate receptor-dependent endocannabinoid mobilization. *Mol Pharmacol* **72**:612–621.
- Kammermeier PJ and Worley PF (2007) Homer 1a uncouples metabotropic glutamate receptor 5 from postsynaptic effectors. *Proc Natl Acad Sci USA* **104**:6055–6060.
- Kammermeier PJ, Xiao B, Tu JC, Worley PF, and Ikeda SR (2000) Homer proteins regulate coupling of group I metabotropic glutamate receptors to N-type calcium and M-type potassium channels. *J Neurosci* **20**:7238–7245.
- Kato A, Ozawa F, Saitoh Y, Fukazawa Y, Sugiyama H, and Inokuchi K (1998) Novel members of the Ves1/Homer family of PDZ proteins that bind metabotropic glutamate receptors. *J Biol Chem* **273**:23969–23975.
- Kato AS, Knierman MD, Siuda ER, Isaac JT, Nisenbaum ES, and Bredt DS (2012) Glutamate receptor  $\delta 2$  associates with metabotropic glutamate receptor 1 (mGluR1), protein kinase C $\gamma$ , and canonical transient receptor potential 3 and regulates mGluR1-mediated synaptic transmission in cerebellar Purkinje neurons. *J Neurosci* **32**:15296–15308.
- Konno K, Matsuda K, Nakamoto C, Uchigashima M, Miyazaki T, Yamasaki M, Sakimura K, Yuzaki M, and Watanabe M (2014) Enriched expression of GluD1 in higher brain regions and its involvement in parallel fiber-interneuron synapse formation in the cerebellum. *J Neurosci* **34**:7412–7424.
- Livide G, Patriarchi T, Amenduni M, Amabile S, Yasui D, Calcagno E, Lo Rizzo C, De Falco G, Olivieri C, and Ariani F et al. (2015) GluD1 is a common altered player in neuronal differentiation from both MECP2-mutated and CDKL5-mutated iPSCs. *Eur J Hum Genet* **23**:195–201.
- Lomeli H, Sprengel R, Laurie DJ, Köhr G, Herb A, Seeburg PH, and Wisden W (1993) The rat delta-1 and delta-2 subunits extend the excitatory amino acid receptor family. *FEBS Lett* **315**:318–322.
- Lujan R, Nusser Z, Roberts JD, Shigemoto R, and Somogyi P (1996) Perisynaptic location of metabotropic glutamate receptors mGluR1 and mGluR5 on dendrites and dendritic spines in the rat hippocampus. *Eur J Neurosci* **8**:1488–1500.
- Mao L, Yang L, Tang Q, Samdani S, Zhang G, and Wang JQ (2005) The scaffold protein Homer1b/c links metabotropic glutamate receptor 5 to extracellular signal-regulated protein kinase cascades in neurons. *J Neurosci* **25**:2741–2752.
- Marchetto MC, Carroneu C, Acab A, Yu D, Yeo GW, Mu Y, Chen G, Gage FH, and Muotri AR (2010) A model for neural development and treatment of Rett syndrome using human induced pluripotent stem cells. *Cell* **143**:527–539.
- Matta JA, Ashby MC, Sanz-Clemente A, Roche KW, and Isaac JT (2011) mGluR5 and NMDA receptors drive the experience- and activity-dependent NMDA receptor NR2B to NR2A subunit switch. *Neuron* **70**:339–351.

- Na ES, Nelson ED, Kavalali ET, and Monteggia LM (2013) The impact of MeCP2 loss- or gain-of-function on synaptic plasticity. *Neuropsychopharmacology* **38**: 212–219.
- Naur P, Hansen KB, Kristensen AS, Dravid SM, Pickering DS, Olsen L, Vestergaard B, Egebjerg J, Gajhede M, and Traynelis SF et al. (2007) Ionotropic glutamate-like receptor delta2 binds D-serine and glycine. *Proc Natl Acad Sci USA* **104**: 14116–14121.
- Nelson ED, Kavalali ET, and Monteggia LM (2006) MeCP2-dependent transcriptional repression regulates excitatory neurotransmission. *Curr Biol* **16**:710–716.
- Niswender CM and Conn PJ (2010) Metabotropic glutamate receptors: physiology, pharmacology, and disease. *Annu Rev Pharmacol Toxicol* **50**:295–322.
- Nord AS, Roeb W, Dickel DE, Walsh T, Kusenda M, O'Connor KL, Malhotra D, McCarthy SE, Stray SM, and Taylor SM et al.; STAART Psychopharmacology Network (2011) Reduced transcript expression of genes affected by inherited and de novo CNVs in autism. *Eur J Hum Genet* **19**:727–731.
- Penzes P, Cahill ME, Jones KA, VanLeeuwen JE, and Woolfrey KM (2011) Dendritic spine pathology in neuropsychiatric disorders. *Nat Neurosci* **14**:285–293.
- Rae MG and Irving AJ (2004) Both mGluR1 and mGluR5 mediate Ca<sup>2+</sup> release and inward currents in hippocampal CA1 pyramidal neurons. *Neuropharmacology* **46**: 1057–1069.
- Ricciardi S, Boggio EM, Grosso S, Lonetti G, Forlani G, Stefanelli G, Calcagno E, Morello N, Landsberger N, and Biffo S et al. (2011) Reduced AKT/mTOR signaling and protein synthesis dysregulation in a Rett syndrome animal model. *Hum Mol Genet* **20**:1182–1196.
- Ronesi JA, Collins KA, Hays SA, Tsai NP, Guo W, Birnbaum SG, Hu JH, Worley PF, Gibson JR, and Huber KM (2012) Disrupted Homer scaffolds mediate abnormal mGluR5 function in a mouse model of fragile X syndrome. *Nat Neurosci* **15**: 431–440.
- Ronesi JA and Huber KM (2008) Homer interactions are necessary for metabotropic glutamate receptor-induced long-term depression and translational activation. *J Neurosci* **28**:543–547.
- Rong R, Ahn JY, Huang H, Nagata E, Kalman D, Kapp JA, Tu J, Worley PF, Snyder SH, and Ye K (2003) PI3 kinase enhancer-Homer complex couples mGluRI to PI3 kinase, preventing neuronal apoptosis. *Nat Neurosci* **6**:1153–1161.
- Schmidt EK, Clavarino G, Ceppi M, and Pierre P (2009) SUnSET, a nonradioactive method to monitor protein synthesis. *Nat Methods* **6**:275–277.
- Shigemoto R and Mizuno N (2000) Metabotropic glutamate receptors immunocytochemical and in situ hybridization analyses, in *Handbook of Chemical Neuroanatomy*, Vol. **18**, pp 63–98, Elsevier, Amsterdam.
- Shiraishi-Yamaguchi Y and Furuichi T (2007) The Homer family proteins. *Genome Biol* **8**:206.
- Smith M, Spence MA, and Flodman P (2009) Nuclear and mitochondrial genome defects in autisms. *Ann N Y Acad Sci* **1151**:102–132.
- Snyder EM, Philpot BD, Huber KM, Dong X, Fallon JR, and Bear MF (2001) Internalization of ionotropic glutamate receptors in response to mGluR activation. *Nat Neurosci* **4**:1079–1085.
- Swanger SA, Yao X, Gross C, and Bassell GJ (2011) Automated 4D analysis of dendritic spine morphology: applications to stimulus-induced spine remodeling and pharmacological rescue in a disease model. *Mol Brain* **4**:38.
- Tu JC, Xiao B, Naisbitt S, Yuan JP, Petralia RS, Brakeman P, Doan A, Aakalu VK, Lanahan AA, and Sheng M et al. (1999) Coupling of mGluR/Homer and PSD-95 complexes by the Shank family of postsynaptic density proteins. *Neuron* **23**: 583–592.
- Uemura T, Mori H, and Mishina M (2004) Direct interaction of GluRdelta2 with Shank scaffold proteins in cerebellar Purkinje cells. *Mol Cell Neurosci* **26**:330–341.
- Vanderklish PW and Edelman GM (2002) Dendritic spines elongate after stimulation of group 1 metabotropic glutamate receptors in cultured hippocampal neurons. *Proc Natl Acad Sci USA* **99**:1639–1644.
- Won YJ, Puhl HL, 3rd, and Ikeda SR (2009) Molecular reconstruction of mGluR5-mediated endocannabinoid signaling cascade in single rat sympathetic neurons. *J Neurosci* **29**:13603–13612.
- Xu J, Zhu Y, Contractor A, and Heinemann SF (2009) mGluR5 has a critical role in inhibitory learning. *J Neurosci* **29**:3676–3684.
- Yadav R, Gupta SC, Hillman BG, Bhatt JM, Stairs DJ, and Dravid SM (2012) Deletion of glutamate delta-1 receptor in mouse leads to aberrant emotional and social behaviors. *PLoS One* **7**:e32969.
- Yadav R, Hillman BG, Gupta SC, Suryavanshi P, Bhatt JM, Pavuluri R, Stairs DJ, and Dravid SM (2013) Deletion of glutamate delta-1 receptor in mouse leads to enhanced working memory and deficit in fear conditioning. *PLoS One* **8**:e60785.
- Yadav R, Rimerman R, Scofield MA, and Dravid SM (2011) Mutations in the transmembrane domain M3 generate spontaneously open orphan glutamate  $\delta$ 1 receptor. *Brain Res* **1382**:1–8.

---

**Address correspondence to:** Dr. Shashank M. Dravid, Department of Pharmacology, Creighton University, School of Medicine, 2500 California Plaza, Omaha, NE 68178. E-mail: ShashankDravid@creighton.edu

---